

Entanglement in One-Dimensional Spin Systems

Andreas Osterloh, Luigi Amico

*MATISS-INFM & Dipartimento di Metodologie Fisiche e Chimiche (DMFCI),
viale A. Doria 6, 95125 Catania, ITALY*

Francesco Plastina, Rosario Fazio

NEST-INFM & Scuola Normale Superiore, I-56127 Pisa, ITALY

For the anisotropic XY model in transverse magnetic field, we analyze the ground state and its concurrence-free point for generic anisotropy, and the time evolution of initial Bell states created in a fully polarized background and on the ground state. We find that the pairwise entanglement propagates with a velocity proportional to the reduced interaction for all the four Bell states. A transmutation from singlet-like to triplet-like states is observed during the propagation. Characteristic for the anisotropic models is the instantaneous creation of pairwise entanglement from a fully polarized state; furthermore, the propagation of pairwise entanglement is suppressed in favor of a creation of different types of entanglement. The “entanglement wave” evolving from a Bell state on the ground state turns out to be very localized in space-time. Our findings agree with a recently formulated conjecture on entanglement sharing; some results are interpreted in terms of this conjecture.

I. INTRODUCTION

A quantum mechanical system possesses additional correlations that do not have a classical counterpart. This phenomenon, called entanglement¹, is probably one of the most astonishing features of quantum mechanics. Understanding the nature of these non-local correlations has been a central issue in the discussion of the foundation of quantum mechanics. More recently, with the burst of interest in quantum information processing, entanglement has been identified as an ingredient for the speed-up in quantum computation and quantum communication protocols² as compared with their classical counterparts. Therefore it is of crucial importance to be able to generate, manipulate and detect entangled states. Experimental efforts in this direction have been put forward using photons³, cavity QED systems⁴, ion traps⁵, and coupled quantum dots⁶. Also encouraged by the advances in the field of nanoscience, there has been a number of proposals to detect signatures of entanglement. Systems under current study are multiterminal mesoscopic devices^{7,8} and Josephson junctions⁹.

Though in many-body systems correlated states naturally appear, a research activity investigating entanglement in condensed matter systems emerged only recently. Despite conceptual difficulties, e.g. in distilling the quantum part of the correlations while the interaction between the subsystems is on, many-body systems might become useful for the development of new computation schemes and/or communication protocols. As an example we mention the recent proposal by Bose¹⁰ to use the spin dynamics in Heisenberg rings to transfer quantum states. It is conceivable that along the same lines other quantum information tasks can be implemented as well.

An important motivation for us to study the interconnection between condensed matter and quantum information is to investigate whether it is possible to gain additional insight in condensed matter states from quantum information theory¹¹. The peculiar aspects of non-local correlations become particularly evident when many bodies behave collectively; a prominent example is a system close to a quantum phase transition¹², where it was found that entanglement can be classified in the framework of scaling theory^{13,14,15,16}, but also profound differences between non-local quantum and classical correlations have been highlighted. In a very recent paper the problem of decoherence in a near-critical one-dimensional system was addressed¹⁷. The study of entanglement has not been devoted only to spin systems, but also to the BCS model^{18,19}, quantum Hall^{20,21} and Boson systems²².

In this paper, we examine the evolution of a local excitation bearing entanglement. There are a number of questions that can be addressed in this way. In particular we would like to see if there

is a well defined velocity for the transport of entanglement and how it is related to the propagation of the elementary excitations of the spin system. Furthermore: is there a parameter regime which favors entanglement transport even over larger distances; what are the time scales for the damping of entanglement created initially. Another important question to analyze is how the transport of entanglement is influenced by the interference with other entangled states. Finally, we try to discriminate pairwise from other types of entanglement. This problem was quantified by Coffman, Kundu, and Wootters (CKW) in terms of a conjecture on a measure for residual entanglement²³.

The paper is organized as follows: In the next section we will introduce the model Hamiltonian, its spectrum and correlation functions needed in the subsequent sections. In section III we present the applied entanglement measures. Section IV is revisiting the ground state entanglement and the entanglement dynamics for the isotropic and anisotropic model is presented in section V. The final section is devoted to conclusions.

II. THE MODEL

The system under consideration is a spin-1/2 ferromagnetic chain with an exchange coupling λ in a transverse magnetic field of strength h . The Hamiltonian is $H = hH_s$ with the dimensionless Hamilton operator H_s being

$$H_s = -\lambda \sum_{i=1}^N (1 + \gamma) S_i^x S_{i+1}^x + (1 - \gamma) S_i^y S_{i+1}^y - \sum_{i=1}^N S_i^z \quad (1)$$

where S^a are the spin-1/2 matrices ($a = x, y, z$) and N is the number of sites. We assume periodic boundary conditions. The anisotropy parameter γ connects the quantum Ising model for $\gamma = 1$ with the isotropic XY model for $\gamma = 0$. In the interval $0 < \gamma \leq 1$ the model belongs to the Ising universality class and for $N = \infty$ it undergoes a quantum phase transition at the critical value $\lambda_c = 1$. The order parameter is the magnetization in x -direction, $\langle S^x \rangle$, which is different from zero for $\lambda > 1$ and vanishes at and below the transition. On the contrary the magnetization along the z -direction, $\langle S^z \rangle$, is different from zero for any value of λ .

This class of models can be diagonalized by means of the Jordan-Wigner transformation^{24,25,26,27} that maps spins to one dimensional spinless fermions with creation and annihilation operators c_l^\dagger and c_l . It is convenient to use the operators $A_l := c_l^\dagger + c_l$, $B_l := c_l^\dagger - c_l$, which fulfill the anticommutation rules $\{A_l, A_m\} = -\{B_l, B_m\} = 2\delta_{lm}$, $\{A_l, B_m\} = 0$. In terms of these operators the Jordan-Wigner transformation reads $S_l^x = \frac{1}{2} A_l \prod_{s=1}^{l-1} A_s B_s$, $S_l^y = -\frac{i}{2} B_l \prod_{s=1}^{l-1} A_s B_s$, and $S_l^z = -\frac{1}{2} A_l B_l$. The Hamiltonian defined in Eq.(1) is bilinear in the fermionic degrees of freedom and is diagonalized by means of the transformation $\eta_k = \frac{1}{\sqrt{N}} \sum_l e^{ikl} [\alpha_k c_l + i\beta_k c_l^\dagger]$ with coefficients $\alpha_k = \frac{\Lambda_k - (1 + \lambda \cos k)}{\sqrt{2[\Lambda_k^2 - (1 + \lambda \cos k)\Lambda_k]}}$ and $\beta_k = \frac{\gamma \lambda \sin k}{\sqrt{2[\Lambda_k^2 - (1 + \lambda \cos k)\Lambda_k]}}$. The Hamiltonian then has the form

$$H = \sum_k \Lambda_k \eta_k^\dagger \eta_k - \frac{1}{2} \sum_k \Lambda_k ; \quad \Lambda_k = \sqrt{(1 + \lambda \cos k)^2 + \lambda^2 \gamma^2 \sin^2 k} . \quad (2)$$

A. Correlation functions

As specified within the next section, one- and two site- entanglement measures are obtained from the (one- and two-body) reduced density matrix whose entries can be related to various spin correlation functions

$$M_l^\alpha(t) = \langle \psi | S_l^\alpha(t) | \psi \rangle ; \quad g_{lm}^{\alpha\beta}(t) = \langle \psi | S_l^\alpha(t) S_m^\beta(t) | \psi \rangle . \quad (3)$$

These can be recast in the form of Pfaffians^{26,27,28}. Correlators defined in Eq.(3) have been calculated for this class of models in the case of thermal equilibrium^{24,25,26,27}. In this case, the expression

for the correlators reduces to the calculation of Toeplitz determinants. This is not the case here, since the initial state $|\psi\rangle$ is not an eigenstate of the Hamiltonian Eq.(1). The correlation functions needed here have been obtained in^{29,30}.

As initial state we consider two sites in a Bell state and all other spins being in the state $|\downarrow\rangle$ (or $|\uparrow\rangle$)

$$|\Psi_{i,j}^\varphi\rangle = \frac{1}{\sqrt{2}} \left(c_i^\dagger + e^{i\varphi} c_j^\dagger \right) |\Downarrow\rangle \quad (4)$$

where the vacuum state is defined as $|\Downarrow\rangle = |\downarrow \dots \downarrow\rangle$. This initial state explicitly breaks the translational invariance. The correlators $\langle \Psi_{i,j}^\varphi | S_l^\alpha S_m^\beta | \Psi_{i,j}^\varphi \rangle$ can be expressed as a *sum of Pfaffians* as described in^{29,30} and allow, together with the magnetization, to evaluate the two-body reduced density matrix. Inaccessible by the above technique is the correlation $\langle \pm | S_l^x | \pm \rangle$. However, if $\langle \pm | S_l^{x,y}(t=0) | \pm \rangle = 0$, then it will remain zero during the subsequent evolution due to the parity symmetry of the Hamiltonian. We will consider exclusively this case in the present work. In the case $\gamma = 0$ the particle number conservation leads to a considerable simplification since the vacuum is an eigenstate and the correlation functions can be evaluated directly without resorting on Pfaffians. For an open-ended isotropic chain dynamic correlators have been studied employing the pfaffian expression³¹.

III. MEASURES OF ENTANGLEMENT

On a qualitative basis entanglement is well understood. Both for distinguishable particles (e.g. spins on a lattice) and identical particles (e.g. free fermions/bosons).³² If a many-spin system is in a pure state, a rough measure for the entanglement between two subsystems is the *mixedness* of the reduced density matrix of the subsystem. We analyze the case when this subsystem is a single site and choose the one-tangle, which on site j is given by

$$\tau^{(1)}[\rho^{(1)}] := 4\det\rho^{(1)} = \frac{1}{4} - \langle S_j^z \rangle^2.$$

Bipartite entanglement is encoded in the two-qubit reduced density matrix $\rho^{(2)}$, obtained from the wave-function of the state after all the spins except those at positions i and j have been traced out. The resulting $\rho^{(2)}$ represents a mixed state of a bipartite system for which a good deal of work has been devoted to quantify its entanglement^{33,34,35}. As a measure for mixed states of two qubits, we use the concurrence³⁶ $C[\rho^{(2)}]$

$$C[\rho^{(2)}] := \max\{0, 2\lambda_{max} - \text{tr}\sqrt{R}\}; \quad R := \rho^{(2)}\sigma_y \otimes \sigma_y \rho^{(2)*}\sigma_y \otimes \sigma_y \quad (5)$$

where λ_{max} is the largest eigenvalue of the matrix \sqrt{R} . For pure two-qubit states we have $\tau^{(1)} \equiv C^2 =: \tau^{(2)}$. The concurrence, expressed in terms of spin correlation functions, is²⁹

$$C_{lm} = 2 \max \left\{ \sqrt{(g_{lm}^{xx} \mp g_{lm}^{yy})^2 + (g_{lm}^{xy} \pm g_{lm}^{yx})^2} - \sqrt{(\frac{1}{4} \mp g_{lm}^{zz})^2 - \frac{1}{4}(M_l^z \mp M_m^z)^2}, 0 \right\} \quad (6)$$

In the isotropic case, additional constants of the motion simplify the expression for the concurrence²⁹. One- and two- site entanglement do not furnish a complete characterization of the entanglement present in spin chains. Following a conjecture put forward by Coffman, Kundu, and Wootters as follows

$$\sum_{j \neq n} C_{n,j}^2 \leq 4 \det \rho_n^{(1)} = \tau_n^{(1)}. \quad (7)$$

it is interesting to study the difference of the quantities in Eq. (7), interpreted as “residual tangle”, i.e. entanglement not stored in two-qubit entanglement. This inequality was proved in Ref.²³ for a three qubit system, giving rise to the definition of the three-tangle as a measure of three-qubit entanglement.

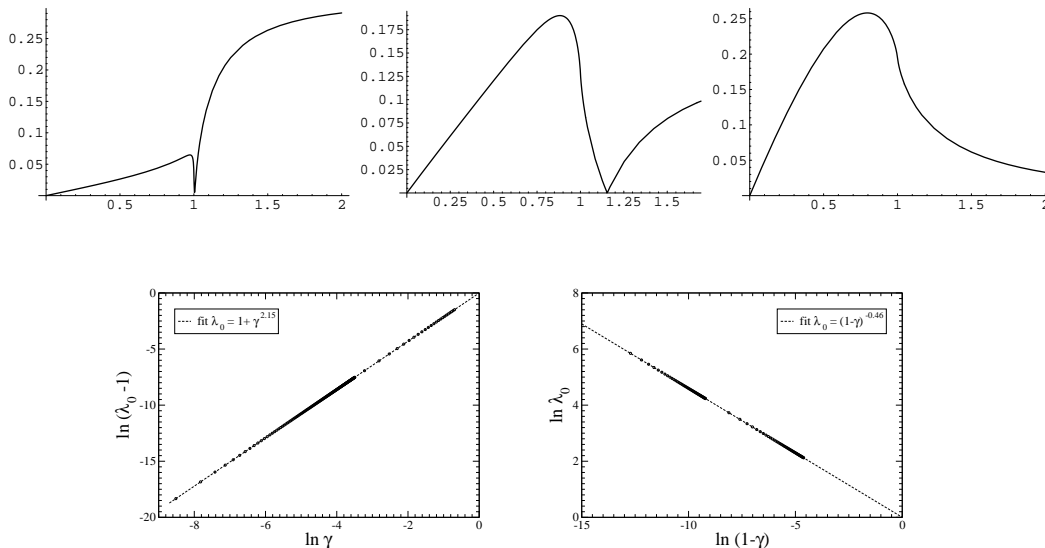


FIG. 1: *Top panel:* The nearest neighbor concurrence C_1 for the values of $\gamma = 0.1, 0.5$, and 1 (from left to right). At $\lambda = 0.5$ and $\lambda = 1$, C_1 has roughly the same value: 0.0264 and 0.0337 for $\gamma = 0.1, 0.1204$ and 0.1285 for $\gamma = 0.5$; 0.2074 and 0.1946 for $\gamma = 1$, respectively. For the Ising model at $\lambda = 0.9$ we have $C_1 = 0.24$. These values remain as uniform background in the concurrence of the singlet-type perturbation of the ground state (see bottom panel of Fig. 5). *Bottom panel:* The behavior of the separable point for generic γ for *left:* $\gamma \rightarrow 0$ and *right:* $\gamma \rightarrow 1$.

IV. GROUND STATE ENTANGLEMENT

This section focuses on the ground state entanglement. In Fig. 1, upper panel, the nearest neighbor concurrence for the ground state is shown for different values of γ as a function of the reduced coupling λ . All exhibit a logarithmic divergence of the first derivative respect to λ at the quantum critical point $\lambda_c = 1$, and fit within finite size scaling theory.¹³ This observation also applies to the first non-zero derivative of the concurrence at larger distance. The cusp, where C_1 vanishes is the point where the large eigenvalues of R , Eq.(5), for the invariant sectors (due to the parity symmetry) $|M_z| = 0$ and $|M_z| = 1/2$ are equal. This indicates a change in the type of Bell state responsible for the entanglement. The value λ_0 where this degeneracy occurs (and the 2-qubit reduced density matrix is separable) converges from above to the critical coupling $\lambda_c = 1$ for $\gamma \rightarrow 0$ as $\lambda_0 = 1 + \gamma^{2.15}$ and diverges as $\gamma \rightarrow 1$ as $\lambda_0 = (1 - \gamma)^{-0.46}$ (see Fig. 1). In the ordered region, the thermal ground state is a mixed state and as a consequence, the here shown concurrence is only an upper bound for the thermal ground state with spontaneously broken symmetry. However, it has been shown recently³⁷ that if it is the triplet sector that furnishes the largest eigenvalue of R , the concurrence is not affected by the thermal mixing. Therefore, the symmetry breaking does not affect the concurrence for $1 \leq \lambda \leq \lambda_0$.

The one-tangle for the ground state is shown on the left of figure 2. At the critical point for $\gamma \in [0.1, 1]$ we could demonstrate that the sum of the two-tangles is much below the one-tangle. This is seen in the right plot of figure 2. If the CKW conjecture holds, this indicated that far the most entanglement is stored in higher tangles (yet to be quantified). This indication recently found further support coming from other indicators for higher entanglement as the scaling of the von Neumann entropy of a compact block of spins with the size of the block¹⁵ and the amount of localizable entanglement, quantified by the maximum two-point correlation function³⁸.

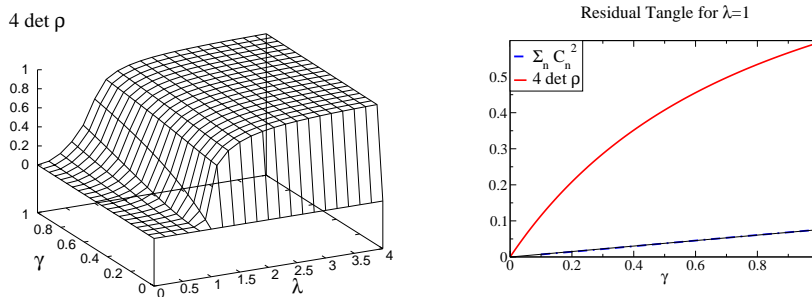


FIG. 2: The global tangle for the groundstate (left). For $0.1 \leq \gamma \leq 1$ we could verify the CKW conjecture for critical coupling (right). The one-tangle (thick line) is much larger than $\sum_{n=-\infty}^{\infty} C_n^2 = 2 \sum_{n=1}^{\infty} C_n^2$ (thick dash-dotted line) suggesting that the major part of entanglement should be stored in higher than two-qubit entanglement. The thin line is a guide to the eye showing that the sum of the two-tangles linearly tends to zero as $\gamma \rightarrow 0$.

V. DYNAMICAL EVOLUTION OF AN E-BIT

The key to the time evolution of the original spin operators is that of the spinless fermions $c_j(t) = \sum_l [\tilde{a}_{l-j}(t)c_l - \tilde{b}_{l-j}(t)c_l^\dagger]$, where the new coefficients are $\tilde{a}_x(t) = \frac{1}{\sqrt{N}} \sum_k \cos kx (e^{i\Lambda_k t} - 2i\beta_k^2 \sin \Lambda_k t)$ and $\tilde{b}_x(t) = \frac{2i}{\sqrt{N}} \sum_k \sin kx \alpha_k \beta_k \sin \Lambda_k t$. In the limit $\gamma = 0$ the previous expressions simplify considerably. In this case the magnetization, i.e. the z -component of the total spin $S^z = \sum_j S_j^z$, is a conserved quantity. In terms of fermions this corresponds to the conservation of the total number of particles, $N = \sum_j n_j = \sum_j c_j^\dagger c_j$. For $\gamma \rightarrow 0$ and $|\lambda| \leq 1$ we find that $\alpha_k \rightarrow 0$ and $\beta_k \rightarrow \text{sign } k$. The energy spectrum is $\Lambda_k = |1 + \lambda \cos k|$ and the eigenstates are plane waves $c_j(t) = \frac{1}{\sqrt{N}} \sum_k \sum_l \cos k(l-j) e^{-i\Lambda_k t} c_l$ and $\eta_k^\dagger = \frac{1}{\sqrt{N}} \sum_l e^{-ikl} c_l$.

A. $\gamma = 0$: The isotropic model

In this section, we describe the dynamics of entanglement for $\gamma = 0$. The Hamiltonian of Eq.(1) is then reduced to the XY model. Only in this case the z -component of the total spin, S^z , is conserved. Consequently the Jordan-Wigner transformed fermionic Hamiltonian becomes a tight binding model for each sector with fixed S^z .

1. Propagation of states in the singlet sector

We first consider the case of a chain initially prepared in a maximally entangled singlet-like state $|\Psi_{i,j}^\varphi\rangle$ on sites i and j as defined in Eq. (4). The state vector at later times is $|\Psi_{i,j}^\varphi\rangle = \sum_l w_l(t) c_l^\dagger |\downarrow\rangle$ with $w_l(t) = \frac{1}{\sqrt{2N}} \sum_k [e^{\frac{2\pi i k}{N}(i-l)} + e^{i\varphi} e^{\frac{2\pi i k}{N}(j-l)}] e^{i\Lambda_k t}$.²⁹ For an infinite system, the coefficients become (up to a global phase) $w_l(t) = \frac{1}{\sqrt{2}} \{J_{i-l}(\lambda t) + e^{i\varphi} (-i)^{(j-i)} J_{j-l}(\lambda t)\}$, where $J_n(x)$ is the Bessel function of order n . For this initial singlet-like state the concurrence of sites n and m is $C_{n,m}(t) = 2|w_n(t)w_m^*(t)|$. The time scale is set up by the interaction strength: the information exchange or “entanglement propagation” takes the time $t \sim d/\lambda$ for d lattice spacings; i.e. the speed of propagation is λ . The propagation of an EPR-like pair is demonstrated in Fig.3, where the concurrence is shown between two sites symmetrically displaced with respect to the initial excitation

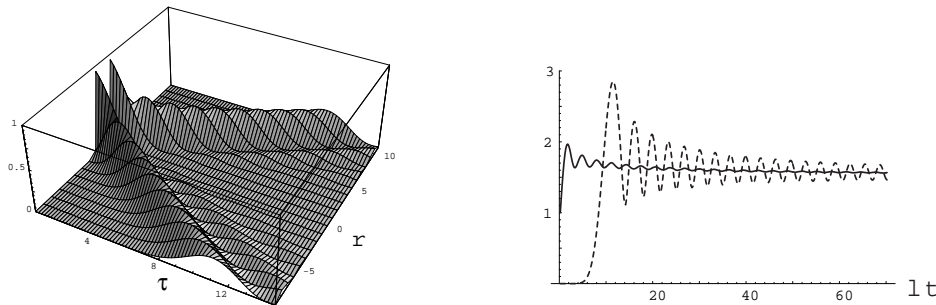


FIG. 3: *Left*: Concurrence between sites $n = -r, m = r$, symmetrically displaced from their initial position $i = -1$ and $j = 1$ ($\varphi = \pi$). *Right*: Summed concurrences for an initially entangled site ($n = 0$, full line) and an initially unentangled site ($n = 10$, dashed line). The initial state is a singlet ($\varphi = \pi$) created on sites $i = 0$ and $j = 1$.

($C_{r,-r}(t)$ for $i = -j = 1$) together with the sum of concurrence $C_{tot,n} = \sum_m C_{n,m}$ of the single site n . The latter tends to the same stationary value (around 1.6) for arbitrary n , independently of the initial conditions²⁹. This means that the initial state becomes homogeneously spread at long times and so does the concurrence.

The same structure as for the concurrence is also found for the one-tangle. This fits within the picture suggested by the CKW conjecture²³. For the isotropic model it is possible to analytically check this conjecture. We obtain $4 \det \rho_j^{(1)} = 4|w_j|^2(1 - |w_j|^2)$ and $\sum_{n \neq j} C_{j,n}^2 = 4 \sum_{n \neq j} |w_j w_n^*|^2 = 4|w_j|^2(1 - |w_j|^2)$. This has already been observed for these W-type states²³. Thus, the two quantities coincide, meaning that the entanglement present in the system is restricted to the class of pairwise entanglement, and no higher order entanglement is created. Therefore, the information in the one-tangle is already contained in the concurrence.

In order to gain information on what type of Bell state propagates and on eventual state mutation, we study how similar is the mixed state $\rho_{n,m}^{(2)}$ to the initial $|\Psi^\varphi\rangle$. This similarity is quantified by the fidelity

$$F_{n,m}(t) = \text{Tr} \left\{ \rho_{n,m}^{(2)}(t) |\Psi^\varphi\rangle \langle \Psi^\varphi| \right\} = \frac{1}{2} |w_n(t) + e^{-i\varphi} w_m(t)|^2. \quad (8)$$

It was shown to display in-phase oscillation with respect to one-tangle and concurrence²⁹. Thus, when the entanglement wave arrives, $\rho_{n,m}^{(2)}$ becomes more similar to the initially prepared state. That means that the state itself is propagating along the chain, taking with it its entanglement. This propagation is far from being a perfect transmission, due to the entanglement sharing with many sites at a time.

2. Propagation of states in the triplet sector

We next analyzed the propagation of the state

$$|\Phi_{i,j}^\varphi\rangle = \frac{1}{\sqrt{2}} (\mathbf{1} + e^{i\varphi} c_i^\dagger c_j^\dagger) |\Downarrow\rangle. \quad (9)$$

These are not single-particle states and since they are superpositions of components pertaining to different spin sectors, one cannot take full advantage of the conservation of the magnetization. As a result, the concurrence is given by $C = \max\{0, C^{(1)}, C^{(2)}\}$; a concurrence of the form $C^{(2)}$ indicates that $|\Psi\rangle$ -like correlation arises, while for $C^{(1)} > C^{(2)}$ the correlations between the two selected sites is more $|\Phi\rangle$ -like. This already suggests that changes in the propagated type of entanglement could

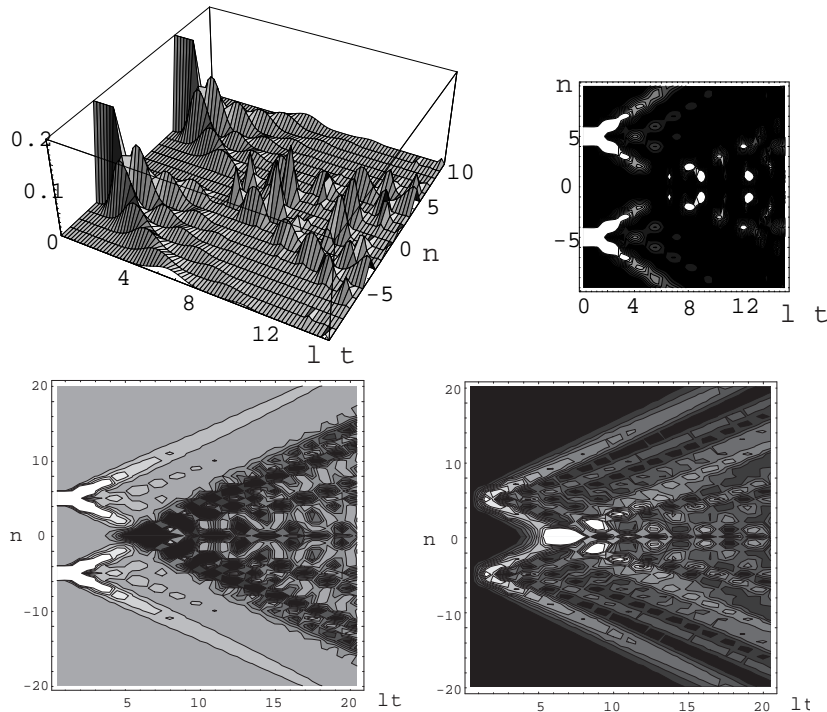


FIG. 4: *Upper panel:* Time evolution of the concurrence between sites $-n$ and n for the initial state $|\Phi_{-5,5}^{\varphi}\rangle$. The plot is cut at 0.2 in order to make the revival after the crossing visible. *Lower panel:* Fidelity (white:high, black:low) of the states $|\Phi^{\varphi_{opt}}\rangle$ (left) and $|\Psi^{\varphi_{opt}}\rangle$ (right) in the density matrix $\rho_{-n,n}^{(2)}(t)$ for the same initial condition as above.

occur.

The entanglement still propagates with the sound velocity $\sim \lambda$ along the chain, as can be seen in Fig. (4), where $C_{-n,n}$ is displayed for an initial state $|\Phi_{-5,5}^{\varphi}\rangle$. At the intersection between the sites of the initial Bell state a revival takes place, and the entanglement then also spreads out from this intersection point. In contrast to the previous case, when the two initially entangled sites are separated by an odd number of spins, the propagating quantum correlations change character. This is seen from the fidelity of the Bell states $|\Phi_{m,n}^{\varphi}\rangle$ and $|\Psi_{m,n}^{\varphi'}\rangle$ in the time evolution of the initial Bell state $|\Phi_{i,j}^{\varphi}\rangle$. These two fidelities are maximized by a proper choice of the phases²⁹ which depend only on the initial and final positions i, j, m and n and are shown in the bottom of Fig. (4) – left plot: $|\Phi^{\varphi_{opt}}\rangle$; right plot: $|\Psi^{\varphi_{opt}}\rangle$ – for $i = -j = 5$ and $n = -m$. Since the fidelity of $|\Phi^{\varphi}\rangle$ in the vacuum is 0.5 due to its component $|\downarrow\downarrow\rangle$, it is seen that after the crossing point the state has become $|\Psi\rangle$ -like. In fact, at the single-site crossing, the amplitude for two parallel spins cannot survive and the outgoing states of this scattering event only contain antiparallel spins. If the initially entangled spins are separated by an even number of sites, the crossing involves two sites and the character of the state is preserved.

B. $\gamma \neq 0$: Singlet onto the vacuum

We now study the model for generic γ and infinite chain. In contrast to the previous section, here the complexity of the computation grows with the distance d of the sites because the dimension of the Pfaffian expression for the correlation functions is $2d \times 2d$. For the critical Ising model it turns out to be sufficient considering $d = 1$, since the concurrence vanishes for larger distances. The

initial state is the singlet $|\Psi_{1,2}^\pi\rangle$, Eq. (4).

1. Concurrence

Figure 5 shows the nearest neighbor concurrence for $\gamma = 0.5, 1.0$ (1st and 2nd panel) and $\lambda = 0.5, 1.0$ (left and right, respectively). A rough estimate of the propagation velocity can be taken from the contour lines in the plot. It coincides with the sound velocity, which is roughly λ as for the isotropic model. For increasing γ it slightly decreases for eventually returning to λ ^{29,31,39}. The concurrence on the original singlet position decays quickly and the damping of oscillations is stronger for increasing λ . We notice an instantaneous signal which, sufficiently far away from the initial singlet position is spatially uniform. This phenomenon reflects the creation of entanglement from the vacuum, which is characteristic for the anisotropic XY models. It is originated from the double spin flip operators $\gamma\lambda/2 \sum_i s_i^+ s_{i+1}^+$ (and its Hermitean conjugate), which are absent in the isotropic model. The initial slope and the type of Bell state created agree well with simple perturbative arguments. This pure vacuum signal dies out very quickly. Towards the critical coupling and the Ising model, the damping of the concurrence propagation gets stronger. The vacuum signal survives much longer for medium λ and $\gamma \rightarrow 1$ such that for $\gamma = 0.5$ and $\gamma = 1$ it interferes with the propagating singlet. Although the damping of the propagation becomes stronger at the critical coupling, nevertheless it is of pure dynamic origin and not related to the quantum phase transition, since the initial state is not the ground state (where the critical behaviour is encoded in). Consistently, the damping turned out to be independent of the size of the chain.

The concurrence for $\gamma = 0.5$ is shown in the top pannel of Fig. 5: we see a clear propagation of the concurrence, which is only slightly stronger damped than for the isotropic model, but there is a creation of entanglement from the vacuum. A “shoulder” appears in the singlet peak of $C_{i,i+1}$, i.e. on the original singlet position, which is due to triplet-type entanglement²⁹. The squares of the preconcurrences $C^{(1)}$ and $C^{(2)}$, shown in the 3rd panel of Fig. 5, alike the analysis of the fidelity of the Bell states in the propagating signal²⁹, demonstrate that the propagation is of the same type as the initially created Bell state (here in the singlet sector), whereas the concurrence created from the vacuum is of triplet type. For the transverse Ising model (2nd panel in Fig. 5), the shoulder on the original singlet position and the vacuum creation gets even more pronounced, but all the signals die out much quicker. For $\lambda = 0.5$ one cannot speak any more of a clearly propagating entanglement signal. At the critical coupling, the propagating signal almost completely disappeared. The next-nearest neighbor and next-next-nearest neighbor concurrence are shown in Fig. 6. Both show a narrow wall created from the vacuum, which for $C_3 := C_{x-3,x}$ is broader. C_3 unveils an additional feature: it shows a large contribution at t around 4 at $x = 3$. It indicates an EPR-type propagation, which we observed already for the isotropic model (see Fig. 3). Considering the velocity λ , the time of appearance indicates that the two fragments have to cross first. At and near the critical coupling C_2 and C_3 identically vanish on the domain of the demonstrated plots.

2. The global tangle

Is it possible to understand how the entanglement, originally stored into the singlet, is going to share among all the spins in the chain? In order to get an idea about what might happen, one can study the one-tangle. For small anisotropy parameter, this quantity is qualitatively very similar to the concurrence: there is an entanglement wave, propagating with velocity λ . For growing γ , the wave is suppressed in favor of a homogeneous growth of the one-tangle which saturates on very short timescales. This signal cannot be due to the initial singlet, of course, but it is created from the vacuum. This was confirmed by looking at the total entanglement created solely from the vacuum, i.e. the initial state being the vacuum.²⁹ The right-most plot in Fig.7 shows the residual tangle for the Ising model at $\lambda = 1$; there is no violation of the CKW conjecture.

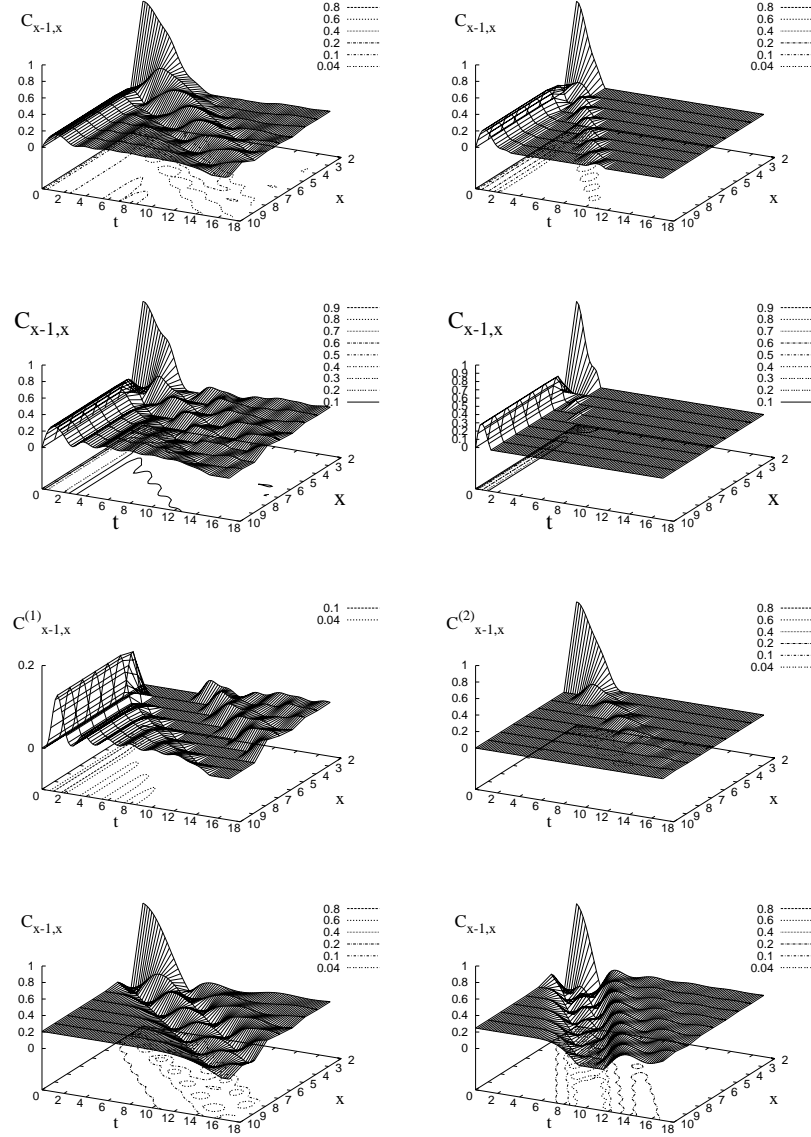


FIG. 5: *Upper two panels:* The nearest neighbor concurrence for medium $\lambda = 0.5$ (left) anisotropy $\gamma = 0.5$ and $\lambda = 0.5$ and 1 (left and right, respectively). The propagation is stronger damped than for small or zero anisotropy. There is a creation from the vacuum which reaches the propagating pulse. At the critical coupling (right), the nearest neighbor concurrence from the initial singlet dies out immediately and so does the vacuum creation. For the Ising model, only few bumps are residues of a propagation. *3'rd panel:* The square of $C^{(1)}$ (left) and $C^{(2)}$ (right) for the Ising model at $\lambda = 0.5$ demonstrate that the propagating signal is in the singlet sector, whereas the background is in the triplet sector. *Bottom panel:* $C_{x-1,x}$ for the perturbed ground state and the Ising model: $\lambda = 0.5$ (left) and $\lambda = 0.9$ (right). There is a background concurrence corresponding to the ground state value (see Fig. 1). A propagating signal is seen in a valley of extinction.

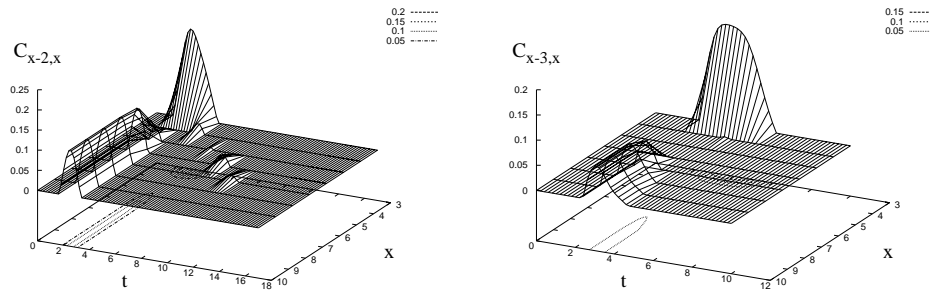


FIG. 6: *Left* - The next nearest neighbor concurrence C_2 for the Ising model far from the critical coupling. It is zero at and close to the critical coupling. *Right* - The next-next nearest neighbor concurrence C_3 for the Ising model far from the critical coupling. Also C_3 vanishes at and close to the critical coupling. At $\lambda = 0.5$ we see a considerably large signal, which is due to an EPR-type propagation of a “split” singlet.

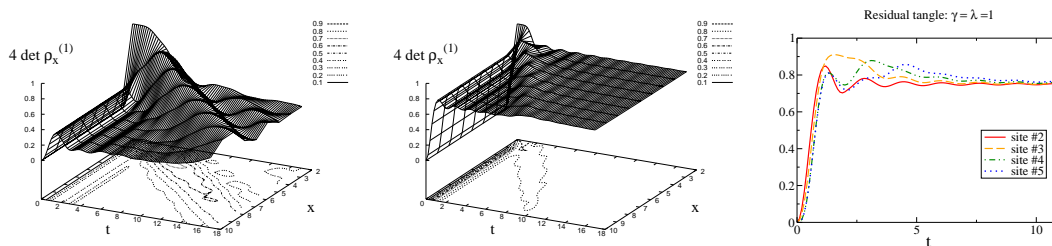


FIG. 7: The total tangle of site x for $\gamma = 1$. In contrast to the nearest neighbor concurrence there is a clear propagating signal here for $\lambda = 0.5$ (left). It is mounted on top of a non-zero background signal coming from the vacuum. At critical coupling (middle) the vacuum background of the one-tangle grows up to about 0.75; the propagation is hardly visible. *Right*: The CKW conjecture applies: the “residual tangle” indeed is positive.

Next, we will study the relative deviations in the one-tangle respect to the time-evolved vacuum

$$\Delta\tau_j^{rel} := 1 - \frac{\det \rho_{(vac)}^{(1)}}{\det \rho_j^{(1)}}. \quad (10)$$

We want to stress that the time evolution operator does not in general preserve the relative order induced by an entanglement measure on the Hilbert space. This manifests in negative values of $\Delta\tau_j$. Eventually, this is due to the fact that superposing (as well as mixing) orthogonal maximally entangled states of the same type diminishes the entanglement. This may lead to a negative $\Delta\tau_j^{rel}$. It is worth noticing that the singlet state is inserted into the vacuum; this is not a superposition of the vacuum and some other state. We choose the same parameter range as above. Along the axis $t = 0$ and $\lambda = 0$ and for site numbers larger than two (and smaller than one) we have that $\det \rho_j^{(1)} = 0$. In these cases, also $\det \rho_{(vac)}^{(1)} = 0$, and we chose the plotted value being zero in these cases. The analysis of $\Delta\tau_j^{rel}$ tells us that for small anisotropy and sufficiently far from the critical coupling the global tangle is dominated by the local perturbation of the vacuum by the singlet (Fig. 8: top), meaning that the total tangle is concurrence dominated. For the isotropic XY model, the global tangle was given entirely by the sum of the 2-tangles such that the CKW-conjecture would conclude that there is no higher tangle contained in the system. In the presence of a small anisotropy, this is no longer true, in particular near to the critical coupling $\lambda = 1$ (Fig. 8). Rising

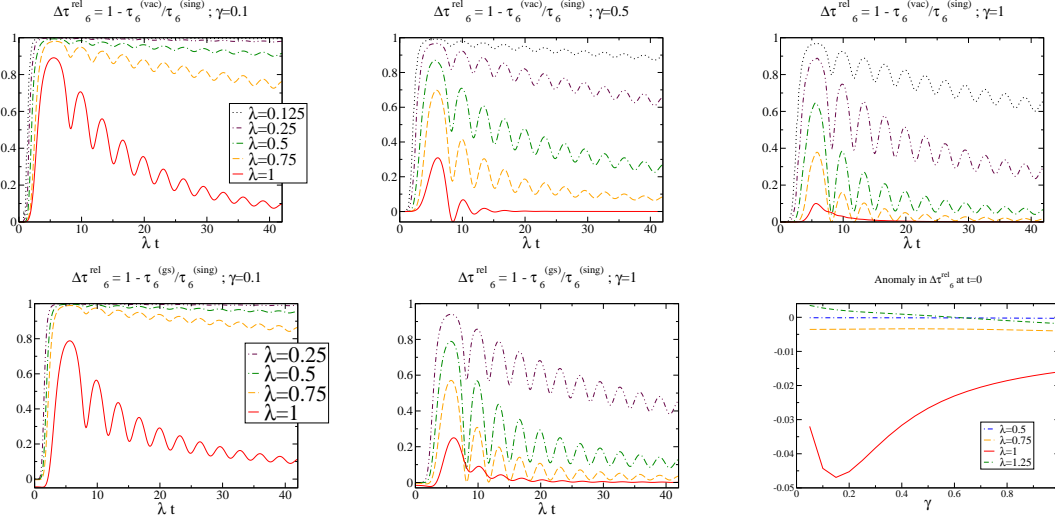


FIG. 8: *Upper panel:* The relative tangle deviation $\Delta\tau_6^{rel}$ from the Vacuum tangle at site number 6 for different values of λ for a fixed value of γ : $\gamma = 0.1$ (left), $\gamma = 0.5$, and $\gamma = 1$ (right). It is plotted as a function of the reduced time $\tau = t/\lambda$; it is nicely seen that the oscillation frequency grows linearly with λ . *Lower panel:* The same as above but for the ground state and $\gamma = 0.1$ (left) and $\gamma = 1$ (center). The oscillation frequency grows linearly with λ . Right: anomaly at $t=0$: it demonstrates the non-local impact of the singlet-type perturbation at the critical coupling.

anisotropy and $\lambda \rightarrow 1$ enhance the vacuum domination.

C. $\gamma \neq 0$: Singlet-type perturbation of the groundstate

One could wonder, whether or not the results in the preceding sections were specific to the vacuum state or what would happen for different states. We therefore discuss in this section the propagation of a singlet-like perturbation of the groundstate $|GS\rangle$, i.e. the time evolution of the initial state

$$|S\rangle_g := \frac{1}{\sqrt{2}}(c_1 - c_2)|GS\rangle. \quad (11)$$

We note that this state differs from a singlet on the ground state since the operators c_i create global excitations. It turned out that the resulting state is nonetheless very similar to the ground state itself²⁹. For the isotropic model $|GS\rangle \equiv |\uparrow\uparrow\rangle$ and hence the dynamics is the same as on the vacuum.

Apart from the propagation of the pulse with velocity about λ , there are several qualitative differences for the concurrence. One of them is that the propagating pulse and the initial Bell state on sites 1 and 2 is the triplet with zero magnetization. This comes from subtleties in the Jordan-Wigner transformation²⁹. The concurrence plots in the bottom panel of Fig. 5 show that the initial state is almost fully entangled on sites 1 and 2. This demonstrates how close is the ground state to $|\uparrow\uparrow\rangle$. Two new features appear in the concurrence signal. Firstly, the entanglement pulse propagates on top of a nonzero background level, which in very good agreement coincides with the nearest neighbor concurrence of the ground state, being around 0.2 at both, $\gamma = 0.9$ and $\gamma = 0.5$ ¹³ (see Fig. 1). This shows that not only is the ground state very close to the vacuum, but that also the state $|S\rangle_g$ is very similar to the ground state as far as nearest neighbor concurrence is considered. Secondly, in contrast to the singlet on the vacuum, we here have to deal with a propagation that eliminates the background concurrence. The latter feature gets more pronounced when approaching the Ising model and critical coupling (see bottom panel of Fig. 5). This elimination is understood

from the fact that joining entanglement of the same type (here: two-site entanglement) in form of states that are orthogonal to those forming the entanglement already present, diminishes the entanglement. Whereas here the impact of the propagating concurrence pulse coming from the initial 0-triplet is the stronger the closer we get to the critical coupling and the quantum Ising model (the opposite of what we observed for the initial singlet onto the vacuum), the situation would be the same as far as the total signal along the propagation line is concerned. This in fact gets more suppressed with growing λ and γ .

For the global tangle we find essentially the same behavior as for the singlet on the vacuum. Only at very short times the singlet-type perturbation diminishes the global tangle. In the bottom panel of Fig 8 we choose two different anisotropies $\gamma = 0.1$ and 1 and compare $\Delta\tau_j^{rel}$ for different couplings λ . The short-time behavior of $\Delta\tau_6^{rel}$ shows a marked anomaly at the critical coupling. This is a cursor of the non-local impact of the singlet-type perturbation of the ground state, which is pronounced at $\lambda_c = 1$. At $\gamma = 0$ all curves should eventually tend to zero.

VI. CONCLUSIONS

In the present work we studied the effect of a singlet-type perturbation on the entanglement of an infinite spin system. We considered quantum XY models for general anisotropy. The dynamics of entanglement was studied as function of the distance to the local perturbation at $t = 0$, and of the reduced interaction strength λ (up to the common quantum critical point of the models at $\lambda = 1$). For this class of models we analyzed a conjecture formulated by Coffman, Kundu, and Wootters quantifying the weight of the pairwise relatively to the global entanglement, measured by $4 \det \rho_1$. In all cases the main propagating signal is in the same sector as that one initially created and the propagation velocity is in good agreement with the sound velocity of the model, which is roughly λ . The isotropic model, i.e. anisotropy $\gamma = 0$, can be mapped onto a tight binding model, and consequently entanglement propagates only, remaining pairwise. In addition we have an EPR-type propagation of the concurrence. We found that states in the triplet sector (with concurrence $C = C^{(1)}$) are mutated after a crossing on a single site. The global tangle and the concurrence (whose square is the 2-tangle) satisfy the Coffman-Kundu-Wootters conjecture with zero residual tangle. This means that *the system contained only pairwise entanglement, measured by the concurrence*. The Hamiltonian does not create any entanglement; it distributes the initially created pairwise entanglement. Also for general anisotropy we found evidence for an EPR-type propagation. The propagation is suppressed, compared to the isotropic model. The suppression is the stronger the closer the system is to the critical coupling and the quantum Ising model. For the latter we found a very rapid damping of the singlet in the nearest neighbor concurrence. For all larger distances we considered (up to 7 lattice spacings) the concurrence is zero. A peculiarity of the anisotropic models is the instantaneous creation of concurrence from the vacuum all over the chain. It decays very quickly when approaching the quantum critical coupling and getting close to the Ising model. Neither effect is of critical origin, though. Comparing quantitatively $4 \det \rho_1$ and concurrence we conclude that *for the anisotropic model the propagation of the concurrence is a small effect respect to the creation of higher tangles*. Medium interaction strengths and/or small anisotropy favor the propagation of the singlet. For the singlet-type perturbation on the ground state, the concurrence signal occurs along a “valley” in the constant background concurrence. The propagating extinction gets more enhanced with growing anisotropy and approaching the critical coupling; for the critical Ising model a weak propagating signal in the valley remains. The background nearest neighbor concurrence coincides with that of the ground state, indicating that the nearest neighbor concurrence away from the initial perturbation is unaffected, and that the Hamiltonian cannot notably create nearest neighbor concurrence beyond that level. The dynamics of the total tangle is basically unchanged. In the short-time behavior of $\Delta\tau_x^{rel}$ an anomaly at $\lambda = 1$ unveils the non-locality of the singlet-type perturbation of the ground state. From the perspective of quantum information, our results can be read as a transfer of a unit of pairwise entanglement (an *e-bit*) within a spin chain by Hamiltonian action. The so transported concurrence can then be distilled at the destination point^{10,40}.

Acknowledgments

The authors would like to thank G. Falci and J. Siewert for helpful discussions. This work was supported by the EU (IST-SQUBIT, RTNNANO), RTN2-2001-00440, and HPRN-CT-2000-00144.

-
- ¹ J. Bell, *Speakable and unspeakable in Quantum Mechanics* (Cambridge University Press, Cambridge, 1987).
 - ² M. Nielsen and I. Chuang, *Quantum Computation and Quantum Communication* (Cambridge University Press, Cambridge, 2000).
 - ³ A. Zeilinger, Rev.Mod.Phys. **71**, 288 (1999).
 - ⁴ A.Rauschenbeutel, G. Nogues, S. Osnaghi, P. Bertet, M. Brune, J.-M. Raimond, and S. Haroche, Science **288**, 2024 (2000).
 - ⁵ C.A.Sackett, D. Kielpinski, B. E. King, C. Langer, V. Meyer, C. J. Myatt, M. Rowe, Q. A. Turchette, D. J. W. W.M. Itano, and C. Monroe, Nature **404**, 256 (2000).
 - ⁶ M. Bayer, P. Hawrylak, K. Hinzer, S. Fafard, M. Korkusinski, Z. R. Wasilewski, O. Stern, and A. Forchel, Science **291**, 451 (2001).
 - ⁷ D. Loss and E. Sukhorukov, Phys. Rev. Lett. **84**, 1035 (2000).
 - ⁸ M.-S. Choi, C. Bruder, and D. Loss, Phys. Rev. B **62**, 13569 (2000).
 - ⁹ F. Plastina, R. Fazio, and G. M. Palma, Phys. Rev. B **64**, 113306 (2001).
 - ¹⁰ S. Bose, quant-ph/0212041 (unpublished) (????).
 - ¹¹ J. Preskill, J. Mod. Optics **47**, 127 (2000).
 - ¹² S. Sachdev, *Quantum Phase Transitions* (Cambridge University Press, Cambridge, 2000).
 - ¹³ A. Osterloh, L. A. G., Falci, and R. Fazio, Nature **416**, 608 (2002).
 - ¹⁴ T. J. Osborne and M. A. Nielsen, Phys. Rev. A **66**, 032110 (2002).
 - ¹⁵ G. Vidal and R. F. Werner, Phys. Rev. A **65**, 032314 (2002).
 - ¹⁶ B.-Q.Jin and V.E.Korepin, quant-ph/0304108 (unpublished) (????).
 - ¹⁷ D. V. Khveshchenko, cond-mat/0301111, (unpublished) (????).
 - ¹⁸ P. Zanardi and X. Wang, J. Phys. A **35**, 7947 (2002).
 - ¹⁹ M. Martin-Delgado, quant-ph/0207026, (unpublished) (????).
 - ²⁰ B. Zeng, H. Zhai, and Z. Xu, Phys. Rev. A **66**, 042324 (2002).
 - ²¹ A. Balachandran, L. Chandar, and A. Momen, Int. J. Mod. Phys. A **12**, 625 (1997).
 - ²² A. P. Hines, R. H. McKenzie, and G. J. Milburn, Phys. Rev. A **67**, 013609 (2003).
 - ²³ V. Coffman, J. Kundu, and W. K. Wootters, Phys. Rev. A **61**, 052306 (2000).
 - ²⁴ E. Lieb, T. Schultz, and D. Mattis, Ann. Phys.(N.Y.) **60**, 407 (1961).
 - ²⁵ P. Pfeuty, Ann. Phys. (N.Y.) **57**, 79 (1970).
 - ²⁶ E. Barouch, B. McCoy, and M. Dresden, Phys. Rev. A **2**, 1075 (1970).
 - ²⁷ E. Barouch and B. McCoy, Phys. Rev. A **3**, 786 (1971).
 - ²⁸ E. R. Caianello and S. Fubini, Nuovo Cimento **9**, 1218 (1952).
 - ²⁹ L. Amico, A. Osterloh, F. Plastina, R. Fazio, and M. Palma, Phys. Rev. A **69**, 022304 (2004).
 - ³⁰ L. Amico and A. Osterloh, J.Phys. A **37**, 291 (2004).
 - ³¹ J. Stolze, A. Noepfert, and G. Mueller, Phys. Rev. B **52**, 4319 (1995).
 - ³² G. Ghirardi, L. Marinatto, and T. Weber, J. Stat. Phys. **108**, 49 (2002).
 - ³³ C. Bennett, H. Bernstein, S. Popescu, and B. Schumacher, Phys. Rev. A **53**, 2046 (1996).
 - ³⁴ V. Vedral, M. Plenio, M. Rippin, and P. Knight, Phys. Rev. Lett. **78**, 2275 (1997).
 - ³⁵ C. Bennett, D. DiVincenzo, J. Smolin, and W. Wootters, Phys. Rev. A **54**, 3824 (1996).
 - ³⁶ W. Wootters, Phys. Rev. Lett. **80**, 2245 (1998).
 - ³⁷ O. F. Syljuasen, Phys. Rev. A **68**, 060301 (2003).
 - ³⁸ J. C. F. Verstraete, M. Popp, Phys. Rev. Lett. **92**, 027901 (2004).
 - ³⁹ A. Noepfert and J. Stolze, private communication.
 - ⁴⁰ M. Horodecki, P. Horodecki, and R. Horodecki, Phys. Rev. Lett. **78**, 574 (1997).